

EFFECTS OF SOURCE DIRECTIVITY AND NONLINEAR SOIL BEHAVIOR  
DURING THE JANUARY, 1 2024 NOTO EARTHQUAKE ( $Mw = 7.5$ )O. V. Pavlenko<sup>\*1</sup> <sup>1</sup> Schmidt Institute of Physics of the Earth, Russian Academy of Sciences, Moscow, Russia

\* Correspondence to: Olga V. Pavlenko, olga@ifz.ru.

**Abstract:** The earthquake of January 1, 2024 with the epicenter at Noto Peninsula of Ishikawa Prefecture, Japan, and the moment magnitude  $Mw = 7.5$  obviously represents an intermediate case between weaker earthquakes with relatively small sources, like the 1995 Kobe and 2000 Tottori earthquakes ( $Mw \sim 6.7-6.8$ ), showing nonlinear soil response and soil softening (reduction of shear moduli) and stronger earthquakes, like the 2003 Tokachi-Oki and Tohoku earthquakes ( $Mw \sim 8.3-9.0$ ) with extended sources and source directivity effects, accompanied by soil hardening and generation of high peak ground accelerations (PGA)  $> 1g$ . In this research, based on KiK-net vertical array records (11 sites), models of soil behavior in the near-fault zones of the 2024 Noto earthquake are constructed, i.e. vertical distributions of stresses and strains in soil layers changing with time during strong motion, which showed nonlinear soil response and reduction of shear moduli in the near-fault zones. At the same time, the waveforms of acceleration time histories indicate the effects of source directivity, when seismic waves, radiated by the crack tip propagated along a rather long section of the fault plane, arrived to remote sites almost simultaneously, overlap, harden subsurface soils and generate high accelerations on the surface, PGA  $\sim 2828$  Gal at remote ISK006 station.

**Keywords:** 2024 Noto earthquake, directivity effects, abnormally high PGA, nonlinear soil behavior.

**Citation:** Pavlenko, O. V. (2024), Effects of Source Directivity and Nonlinear Soil Behavior During the January, 1 2024 Noto Earthquake ( $Mw = 7.5$ ), *Russian Journal of Earth Sciences*, 24, ES2002, EDN: WAAWML, <https://doi.org/10.2205/2024es000909>

## Introduction

Dense networks of seismic observations operating in Japan since 1996, K-NET ( $\sim 1000$  surface instruments) and KiK-net ( $\sim 800$  vertical arrays), provide us with valuable records of strong-motion that allow studying effects of strong earthquakes in the near-fault zones.

The observations indicate that during large earthquakes with extended sources (with moment magnitudes  $Mw \sim 8.0$  and higher), the distributions of peak ground accelerations (PGA) in the near-fault zones usually possess a complicated, mosaic character [NIED, 2024]. During the 2003 Tokachi-oki and 2011 Tohoku earthquakes, maximum PGA exceeding  $\sim 1g$  were recorded at rather large epicentral distances, which is obviously due to the effects of directivity of seismic radiation from extended earthquake sources [Pavlenko, 2017, 2022].

Archuleta and Hartzell were among the first seismologists to draw attention to the effects of directivity [Archuleta and Hartzell, 1981]. Analyzing records of the 1979 Imperial Valley earthquake, where abnormally high accelerations of  $\sim 1195 \text{ cm/s}^2$  were recorded, by means of numerical simulation of high-frequency ground motion, they revealed a strong influence of directivity effects on the acceleration in the near-fault zones [Archuleta and Hartzell, 1981].

As noted by Somerville *et al.* [1997], directivity effects occur when the propagation of a rupture toward a site at a velocity that is almost as large as the shear wave velocity causes most of the seismic energy from the rupture to arrive in a single large pulse of motion, representing the cumulative effect of almost all seismic radiation from the fault. This should be taken into account when predicting the ground motion in the near-fault zones

## RESEARCH ARTICLE

Received: 15 February 2024

Accepted: 11 April 2024

Published: 22 April 2024



**Copyright:** © 2024. The Author.  
This article is an open access article distributed under the terms and conditions of the Creative Commons Attribution (CC BY) license (<https://creativecommons.org/licenses/by/4.0/>).

[Somerville *et al.*, 1997]. Attempts are being made to introduce accounting for directivity effects to seismic hazard assessment [Abrahamson, 2000; Rowshandel, 2006; Shahi and Baker, 2011, etc.].

With the development of strong motion networks and accumulation records of strong earthquakes, the number of observations of directivity effects is increasing. Such effects were observed in Japan, and during the last earthquakes in Turkey on February 6, 2023 ( $M_w \sim 7.5$ – $7.7$ ) the directivity effects were also observed and caused large-scale building destructions [Pavlenko and Pavlenko, 2023; Rosakis *et al.*, 2023]. Evidently, the earthquakes with a moment magnitude  $M_w \sim 7.5$  possess sufficiently large sources for directivity effects to occur.

Such effects were clearly seen on the recordings of stations of Japanese strong-motion networks during large 2003 Tokachi-oki earthquake and 2011 Tohoku earthquake. Abnormally high accelerations ( $> 1$  g) recorded during these earthquakes at stations that were far enough from the epicenter can be explained by the fact that the crack in the earthquake source propagated at a high speed ( $\sim 4$ – $4.3$  km/s) along large parts of the fault plane ( $\sim 100$ – $120$  km) towards these stations, and seismic waves radiated by the crack tip, came to the stations almost simultaneously. Shock wave fronts were formed that gave some additional compression to soil layers beneath the stations, so that amplification of seismic waves in the layers increased, and high PGA on the surface were generated [Pavlenko, 2017, 2022].

During these large earthquakes, nonlinear soil behavior was not as widespread as during the weaker 1995 Kobe and 2000 Tottori earthquakes ( $M_w \sim 6.7$ – $6.8$ ), when significant nonlinearity of the soil response was observed in the near-fault zones [Pavlenko and Irikura, 2003, 2006].

On January 1, 2024, a strong earthquake with a moment magnitude  $M_w \sim 7.5$  struck the northern part of the Noto Peninsula in Ishikawa Prefecture, Japan; it was accompanied by landslides and tsunami of more than 6 meters in height. Figure 1 shows the locations of the epicenter, KiK-net and K-NET stations in the near-fault zones and the estimated boundaries of the fault plane according to USGS. High PGAs  $> 1$  g were recorded throughout the peninsula, with the maximum of  $> 2.8$  g at ISK006 station in its western corner.

As seen from the figure, the Noto earthquake had an extended source, with the length of  $\sim 120$  km, and high PGA at ISK006 site may indicate the effects of source directivity.

Records of KiK-net stations located in near-fault zones allow us to study soil behavior in strong ground motion in order to understand the mechanisms of generation of such high PGA values.

In this research, models of soil behavior during the Noto earthquake are constructed at five KiK-net sites closest to the source plane, such as, ISKH01, ISKH02, ISKH03, ISKH04 and ISKH06 sites. Also, the waveforms of acceleration time histories at sites located in the near-fault zones are analyzed to study possible effects of source directivity and their relation to abnormally high accelerations recorded at ISK006 site.

## Method and data

Tables 1 and 2 present information on the KiK-net and K-NET stations closest to the source of the 2024 Noto earthquake: their coordinates, epicentral distances, ground conditions, i.e., average  $S$ -wave velocities in the upper 10 m and 30 m of soil, and PGA values recorded on the surface. Parameters of the soil profiles are shown in Figure 2.

As seen from the tables, many stations are located on soft soils, including ISH006 station, recorded the highest PGA  $\sim 2828$  Gal: at this site, the upper 8 meters are composed of volcanic ash clay with  $V_s \sim 260$  m/s, and below are denser layers with  $V_s \sim 390$  m/s.

A seismic vertical array KiK-net consists of two three-component accelerometers, one of which is installed on the surface and another in a borehole at a depth of  $\sim 100$ – $120$  m (sometimes more). Strong motion records provided by KiK-net seismic vertical arrays allow us to reconstruct soil behavior in strong ground motion in small time intervals and estimate time-dependent vertical distributions of stresses and strains in the layers from the surface

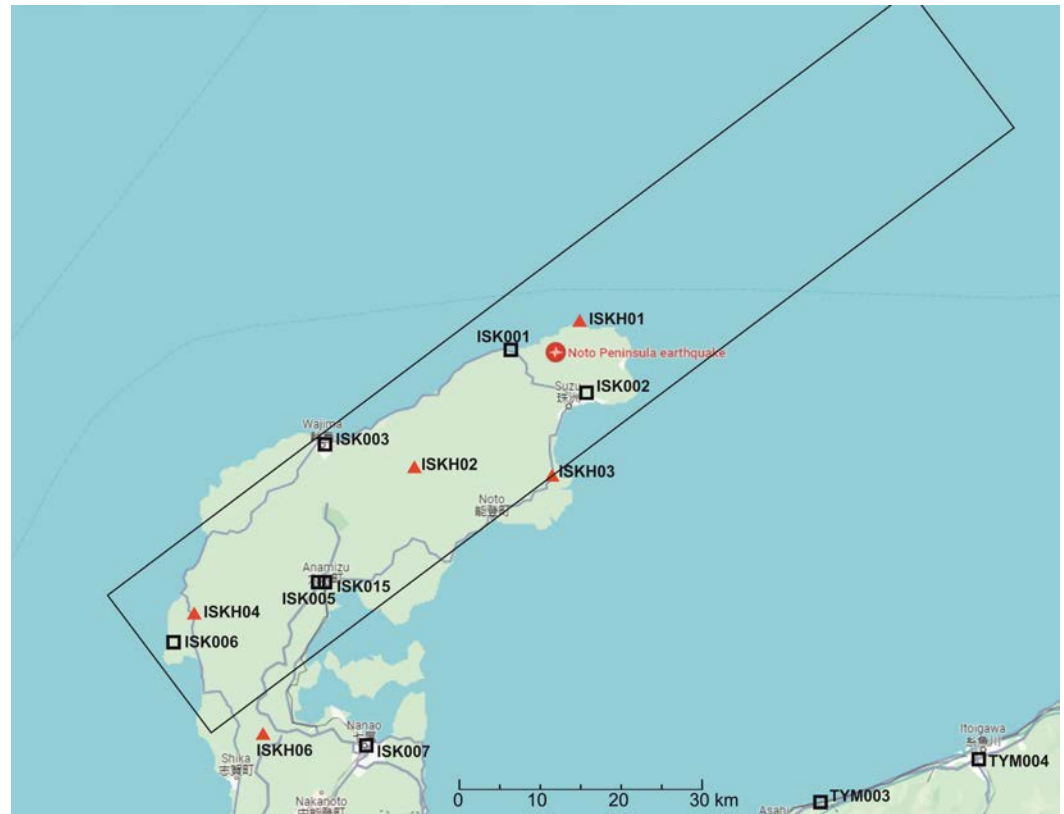


**Figure 1.** Map showing the locations of the 2024 Noto earthquake epicenter (circle), KiK-net (triangles) and K-NET (squares) stations in the near-fault zones and the estimated boundaries of the fault plane.

**Table 1.** Information on the studied KiK-net stations

Site code	Latitude	Longitude	Epicentral distance, km	$V_{s10}$ , m/s	$V_{s30}$ , m/s	PGA, Gal	Borehole depth, m
ISKH01	37.53	137.28	8	261.7	344.9	1006.7	203.5
ISKH03	37.35	137.24	18	171.9	310.9	936.3	210.0
ISKH02	37.36	137.04	21	590.6	720.8	790.8	105.0
ISKH04	37.19	136.72	55	440.0	443.5	1220.5	119.5
ISKH06	37.05	136.82	60	375.0	500.0	803.8	203.45

**Table 2.** Information on the studied K-NET stations

Site code	Latitude	Longitude	Epicentral distance, km	$V_{s10}$ , m/s	PGA, Gal
ISK001	37.5	137.18	2	304.2	1468.7
ISK002	37.45	137.29	10	177.6	917.4
ISK003	37.39	136.91	28	378.2	1632.2
ISK005	37.23	136.90	40	70.9	1279.7
ISK015	37.23	136.91	40	294.7	1000.5
ISK007	37.04	136.97	55	773.9	459.0
ISK006	37.16	136.69	59	278.6	2828.2

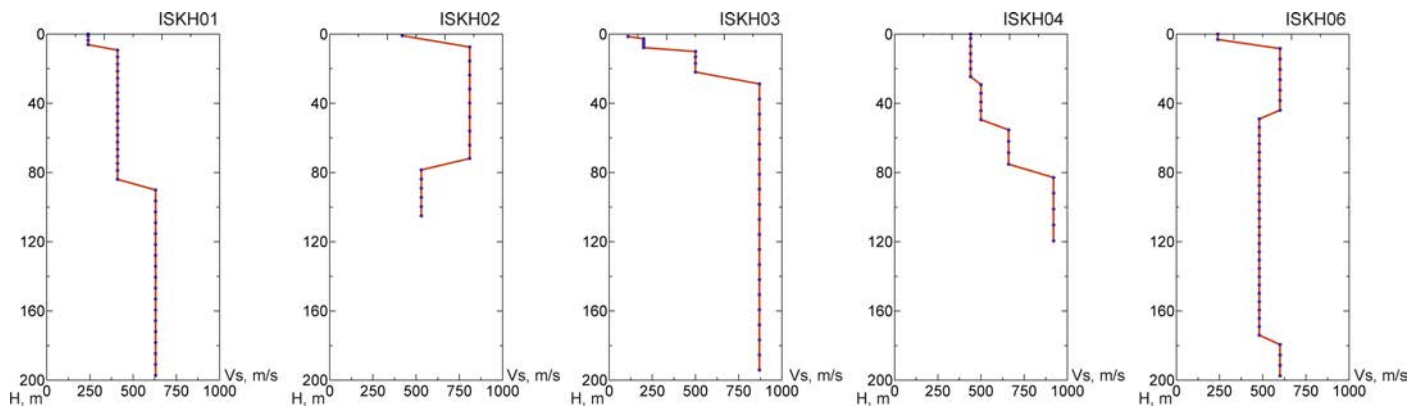


**Figure 2.** Parameters of the soil profiles at the studied KiK-net sites.

down to the location of the deep device. The method was developed by Pavlenko and Irikura and described in detail in [Pavlenko and Irikura, 2003]. It was previously applied to study soil behavior during past strong earthquakes [Pavlenko, 2016, 2022; Pavlenko and Irikura, 2003, 2006]. The constructed models illustrate the behavior of soil layers during strong motion at various time periods.

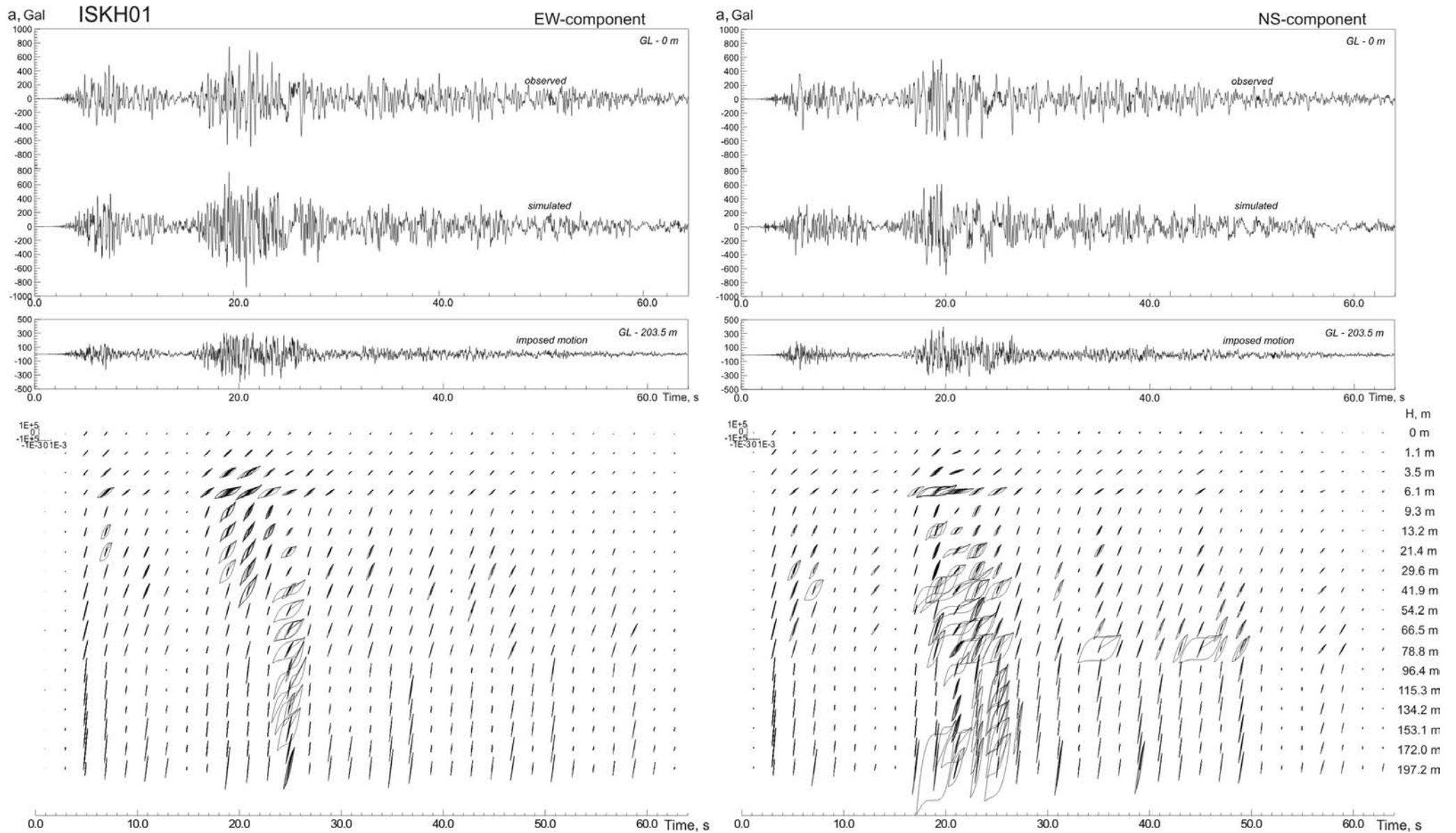
The algorithm of nonlinear analysis by Joyner and Chen [Joyner and Chen, 1975] is used to calculate the propagation of vertically incident shear waves in soil layers. To describe the behavior of soil layers, nonlinear stress-strain relations of soft- or hard- types are used, i.e., relations declining to the strain or to the stress axes at large strains. Series of hysteretic stress-strain curves of various shapes and slopes are generated, and the curves providing the best fit to the records on the surface are selected. Records of deep devices of the vertical arrays are used as input motion to soil columns, and for calculations, they are divided into small time intervals of 2 s duration, to account in temporal changes in soil behavior. Calculations are performed successively, interval by interval. The records were modeled in the frequency range up to 15 Hz.

Parameters of the soil profiles are taken from the website, and soil densities, maximum shear stresses  $\tau_{\max}$ , and attenuation coefficients are selected based on the soil composition and depth, accounting for the lithostatic pressure. The stress-strain relations are normalized in the way proposed by Hardin and Drnevich [1972], i.e., stresses are multiplied by  $1/\tau_{\max}$ , and strains are multiplied by  $G_{\max}/\tau_{\max}$ , where  $\tau_{\max}$  is shear stress in failure, and  $G_{\max}$  is shear modulus in the low-strain range. Differences in the behavior of the layers are due to differences in  $\tau_{\max}$  and  $G_{\max}$  values in the layers. The best-fit relations are selected by the deviations of the simulated accelerograms on the surface from the recorded ones. Thus, soil behavior during strong motion was simulated in 32 two-second intervals (64 s of strong motion).

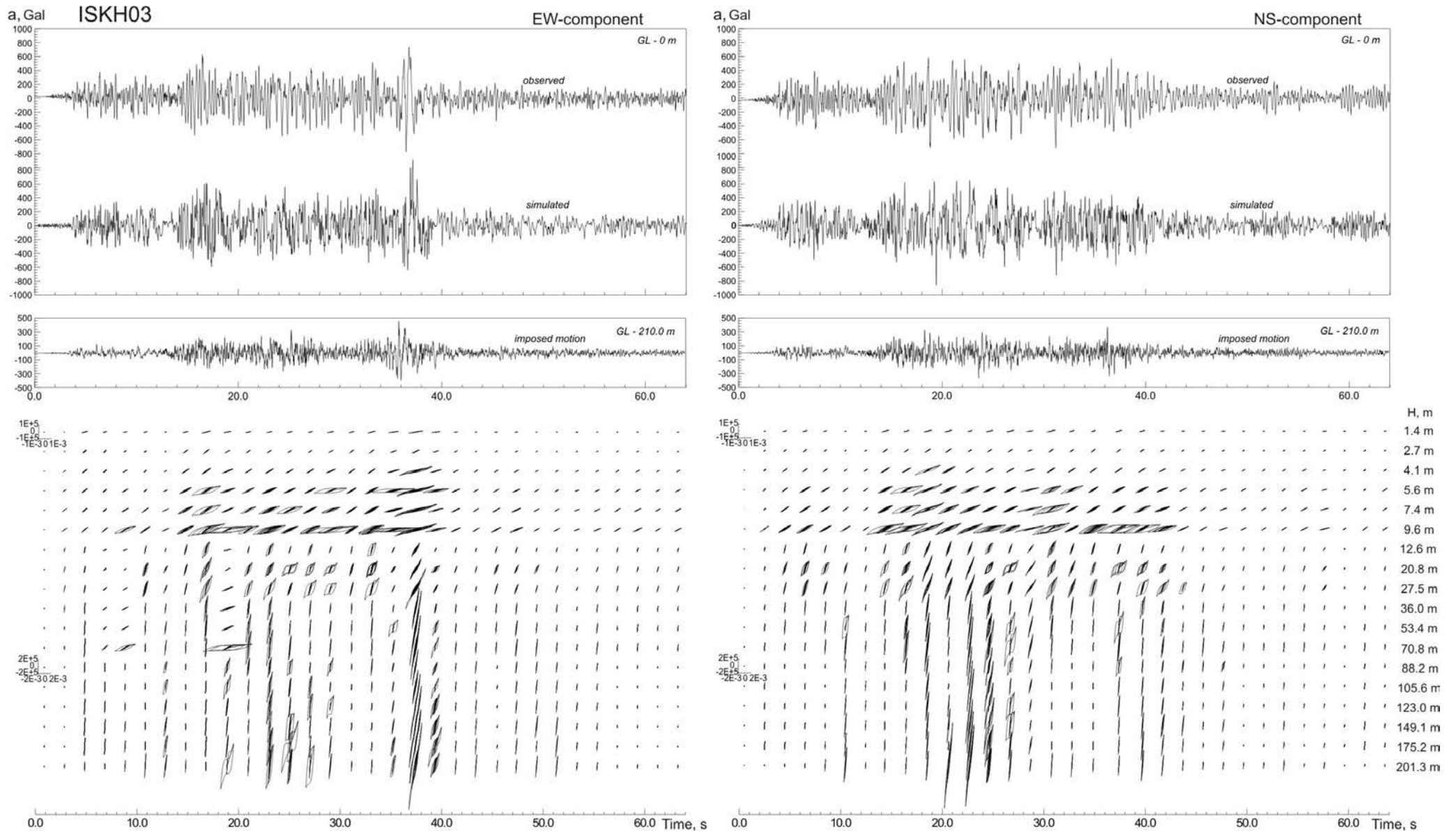
Based on the constructed models, changes of shear moduli in soil layers during strong motion were estimated. Shear moduli were calculated as the ratios of the normalized stresses, averaged over all hysteretic curves within each 2 s time interval, to the normalized strains, averaged in the same manner; then the ratios were averaged over the entire soil thickness, from the surface down to the location of the deep device. To trace the effects of source directivity, changes in the waveforms of the acceleration time histories recorded by K-NET and KiK-net stations in the near-fault zones at various distances from the epicenter were analyzed.

## Results

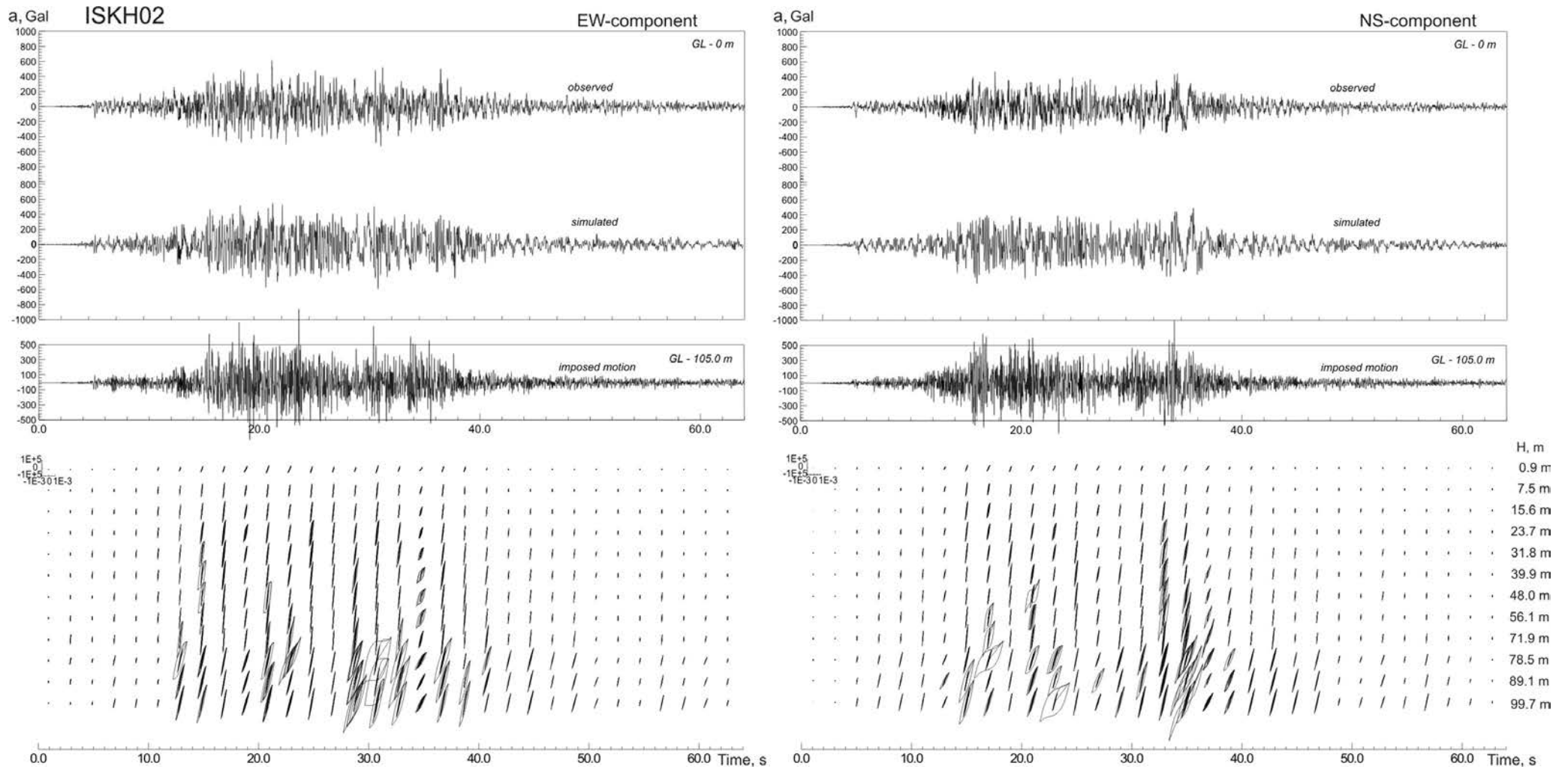
The constructed models of soil behavior during the 2024 Noto earthquake at five KiK-net sites closest to the epicenter are shown in Figure 7 (3–7). As seen from Figure 1, all these sites are located within or just near the projection of the fault plane on the Earth's surface. The estimates of shear moduli in soil layers at these sites, changing with time during strong motion are shown in Figure 4.



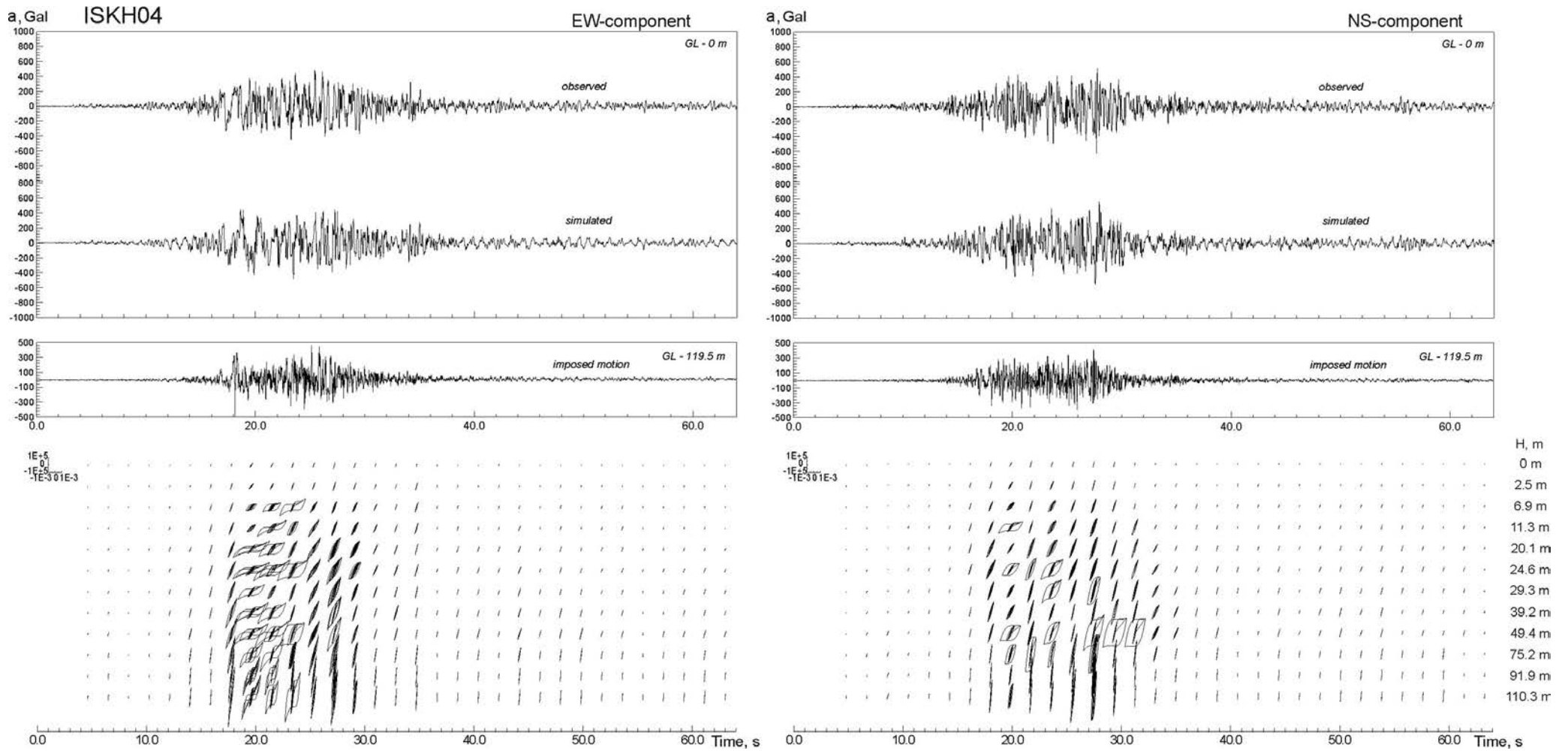
(a) at ISKH01 site.



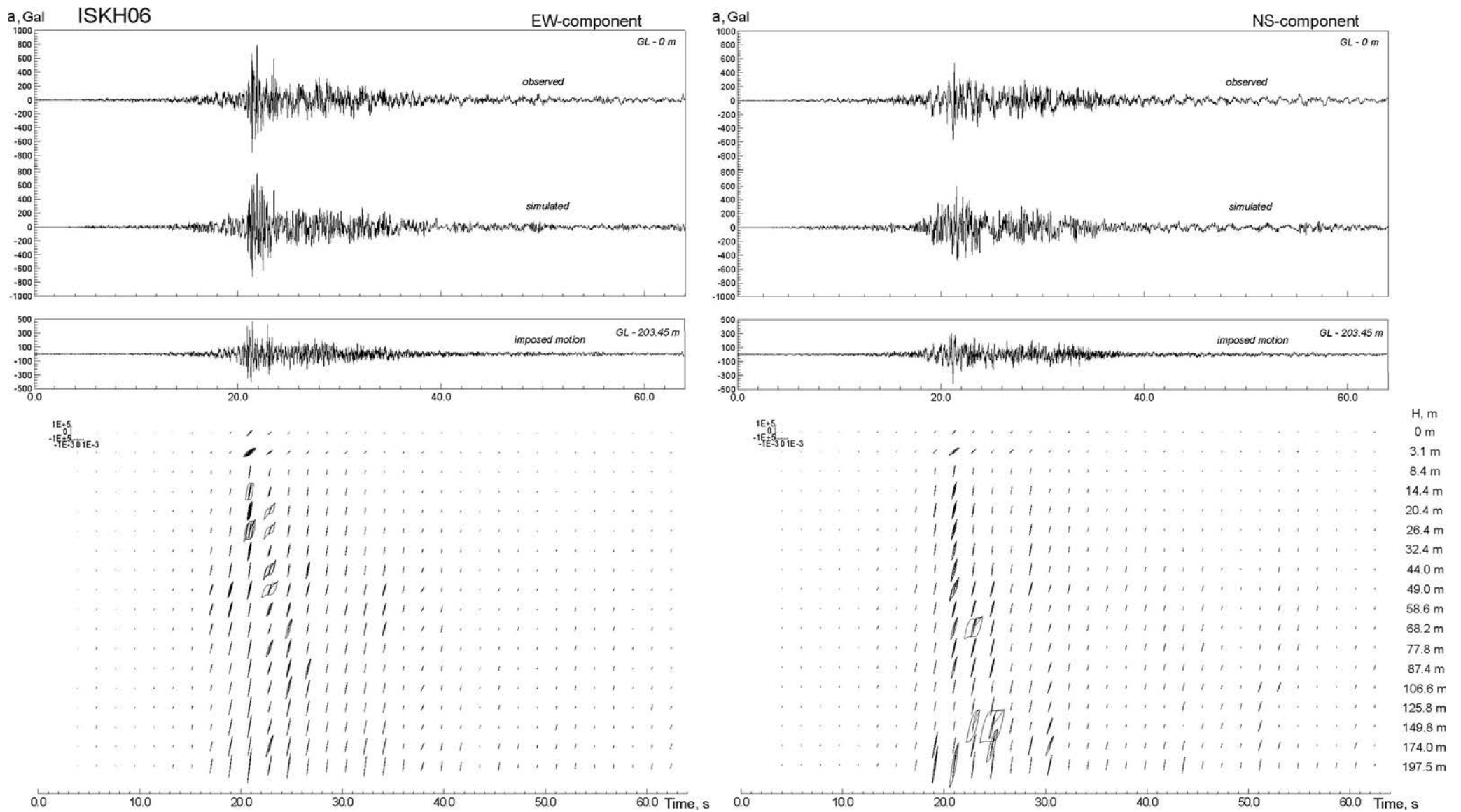
(b) at ISKH03 site.



(c) at ISKH02 site.



(d) at ISKH04 site.



(e) at ISKH06 site.

**Figure 3.** Acceleration time histories of the 2024 Noto earthquake, observed and simulated, and estimated stress-strain relations in soil layers, changing with time during strong motion: a – at ISKH01 site; b – at ISKH03 site; c – at ISKH02 site; d – at ISKH04 site; e – at ISKH06 site. The stresses are given in Pa, and strains in strain.

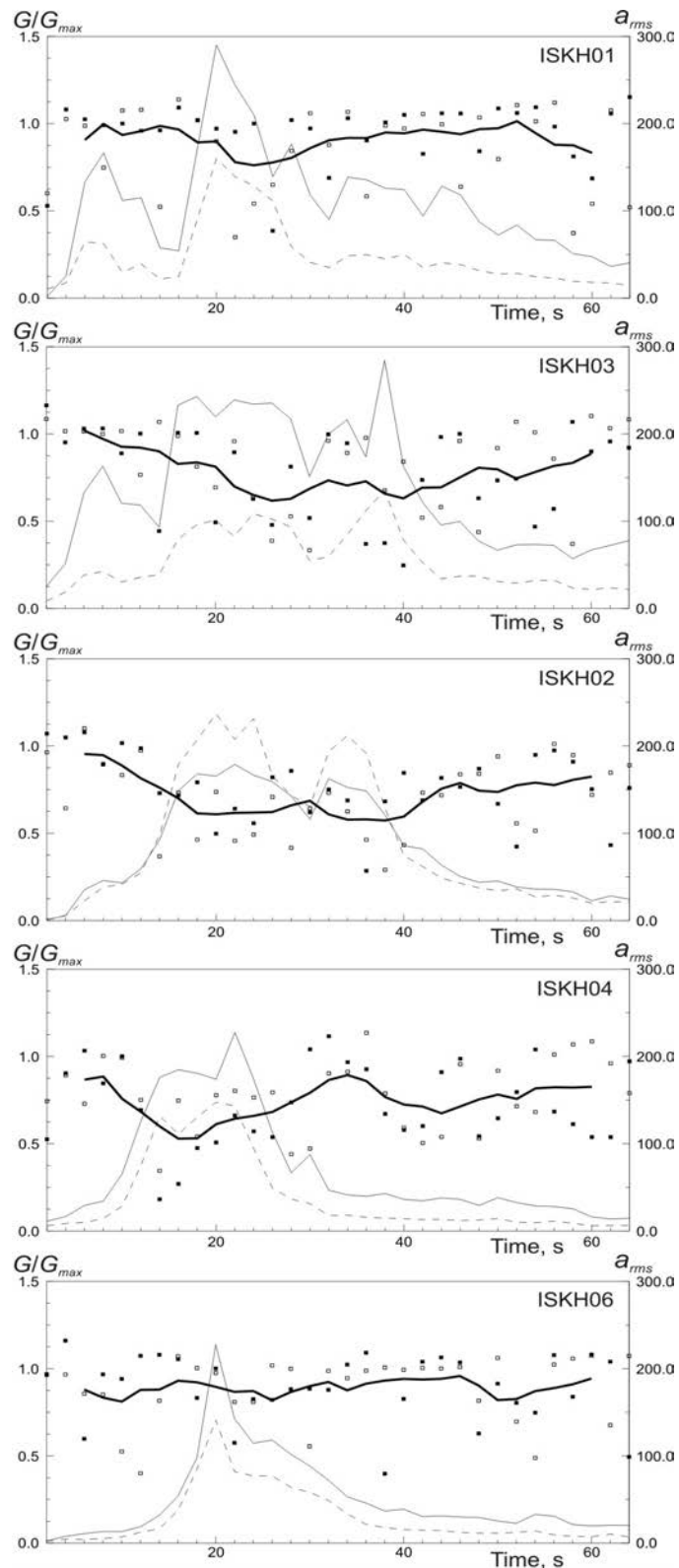


**Figure 4.** Changes of shear moduli in soil layers at the studied KiK-net sites during the 2024 Noto earthquake. Dots are the estimates of shear moduli in successive time intervals (grey and black points correspond to EW and NS components), black lines show these estimates smoothed and averaged over two horizontal components. Thin lines are the intensities of motion (root-mean-square accelerations) on the surface (solid lines) and at depths of locations of the deep devices (dash lines).

The figures show a rather long duration of strong motion at sites closest to the epicenter, which decreases with increasing distance from the epicenter.

At soft-soil stations, such as, ISKH01 and ISKH03 (at epicentral distances of 8 km and 18 km), and at denser-soil stations, such as, ISKH02 and ISKH04 (at epicentral distances of 21 km and 55 km), except the remote ISKH06 station (at epicentral distance of 60 km), we observe substantially nonlinear soil behavior, indicated by nonlinear stress-strain relationships at depths below  $\sim 6$  m at stations ISKH01, ISKH03 and ISKH04 (Figure 7), and reduction and recovery of shear moduli in soil layers during strong motion (Figure 4). At ISKH02 site,  $S$ -wave velocity  $V_s \sim 420$  m/s in the upper 4 m,  $V_s \sim 810$  m/s in the underlying  $\sim 72$  m and decreases to  $V_s \sim 530$  m/s below. The observations show that in such a soil profile, seismic motions do not intensify, but weaken on the surface, and the lower layer ( $V_s \sim 530$  m/s) behaved nonlinearly during strong motion (Figure 5).

At the remote ISKH06 station, the soil behavior was close to linear, and shear moduli in soil layers did not reduce, but remained high during strong motion.

Similar substantially nonlinear soil behavior was observed in the near-fault zones during the 1995 Kobe and 2000 Tottori earthquakes possessing moment magnitudes  $M_w \sim 6.7$ – $6.8$ .

During the stronger 2003 Tokachi-oki ( $M_w \sim 8.3$ ) and 2011 Tohoku earthquakes ( $M_w \sim 9.0$ ), high peak ground accelerations were recorded at rather large distances from the epicenter, and were associated with the effects of directivity of the extended earthquake sources. Nonlinear behavior of soft soils and reduction of shear moduli in soil layers were observed at stations located in the closest vicinity of the fault plane, whereas at a large number of remote stations recorded high PGA exceeding  $> 1$  g, soil behavior was virtually linear. The linearity of soil behavior was due to shock, or Mach fronts, which produced some additional compression to the soil layers, causing soil hardening; shear moduli in soil layers increased and reached their maxima at the moments of the maximum intensity of strong motion, so that high accelerations were recorded on the surface. The effects of directivity were traced by the waveforms of the acceleration time histories: the duration of strong motion decreased with increasing distance from the source, and the wave trains seemed to contract into one point, while peak accelerations did not decrease [Pavlenko, 2017, 2022].

During the 2024 Noto earthquake, abnormally high accelerations were recorded at remote ISK006 station (Table 2), which may also indicate the effects of radiation directivity of the extended earthquake source. At the same time, at KiK-net station ISKH04, closest to ISK006 site, we clearly see a decrease in the duration of strong motion and high PGA, as well as signs of soil hardening, i.e., stress-strain relations in soil layers declining to the vertical axis at the final parts of strong motion (Figure 6) and the corresponding increase of shear moduli, which is not observed at other stations (Figure 4).

Directivity effects during the 2024 Noto earthquake can be traced by changes in the waveforms of the acceleration time histories with increasing distance from the source towards ISK006 site; the waveforms are shown in Figure 5. The fault plane shown in Figure 1, was inclined to the Earth's surface at an angle of  $\sim 45^\circ$ , with its western side located near the surface and its eastern side extending to the depth [Fujii, Yu. and Satake, 2024; Ishikawa, Yu. and Bai, 2024]. So, all the studied stations were located at similar distances from the fault plane. In Figure 5, the stations are arranged in the order of their distance from the epicenter, which can be considered as the projection of the rupture origin to the Earth's surface.

From the figure, we can see a gradual decrease of strong-motion duration with increasing distance from the epicenter, while peak accelerations do not decrease and reach their maximum at ISK006 station, where the duration of strong motion is minimal (ISKH03, ISK015 and ISKH06 stations are located somewhat away from the direction to the ISK006 site, so their waveforms are slightly shifted). This indicates the effects of radiation directivity in the extended source of the Noto earthquake: obviously, the crack propagated along the fault plane from the epicenter to the south-west, towards ISK006 station (Figure 1), so

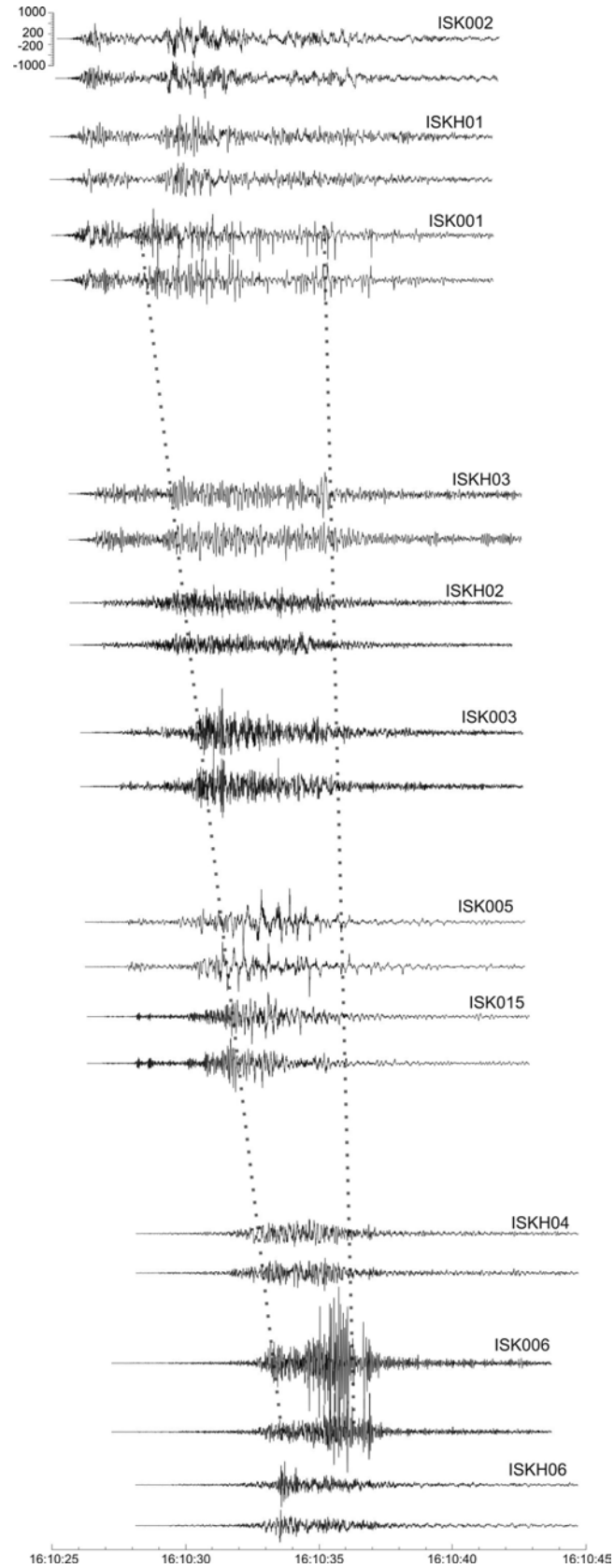


**Figure 5.** Acceleration time histories of the 2024 Noto earthquake (at two horizontal components) recorded by K-NET and KiK-net stations on the surface in the near-fault zones and arranged in ascending order of the epicentral distance (2–60 km).

that seismic waves radiated by the crack tip came to the station almost simultaneously; they overlapped and produced abnormally high PGA  $\sim 2.8g$ . Similar effects were observed during the stronger 2003 Tokachi-oki and 2011 Tohoku earthquakes [Pavlenko, 2017, 2022]; such effects occur due to the velocity structure of the medium, when seismic waves propagate into deeper layers with higher propagation velocities.

Note that the waveforms of the acceleration time histories at K-NET sites ISK005, ISK001 and ISK015 (to a lesser extent) show significant nonlinearity of soil behavior, i.e., spikes in the waveforms, which are usually related to cyclic mobility and soil liquefaction.

### Conclusions

Thus, the near-fault records of the 2024 Noto earthquake show both a significant nonlinearity of soft soil behavior and clear effects of directivity of the extended earthquake source, which produced abnormally high accelerations PGA  $\sim 2.8g$  on the surface.

In this respect, the 2024 Noto earthquake is similar to the 1999 Chi-Chi earthquake ( $M_w \sim 7.6$ ) [Pavlenko, 2008]; both earthquakes evidently represent intermediate cases between weaker earthquakes with magnitudes  $M_w \sim 6.7$ – $6.8$  (like 1995 Kobe and 2000 Tottori earthquakes) that showed substantially nonlinear soft soil behavior in the near-fault zones, and stronger earthquakes with magnitudes  $M_w \sim 8.3$ – $9.0$  (like 2003 Tokachi-oki and 2011 Tohoku earthquakes), the main features of which were directivity effects, shock wave fronts, and predominantly linear soil behavior, with soil hardening and generation of abnormally high PGA.

### Data and Resources

Records of the 2024 Noto earthquake and soil profiling data used in this study are provided by the National Research Institute for Earth Science and Disaster Prevention [NIED, 2024] in Japan, and can be obtained from the Kyoshin and Kiban-Kyoshin Networks.

**Acknowledgments.** I thank the K-NET and KiK-net Digital Strong-Motion Seismograph Network of Japan for the records of the 2024 Noto earthquake and the profiling data. The work was supported by RSF grant 23-27-00316.

### References

- Abrahamson, N. A. (2000), Effects of rupture directivity on probabilistic seismic hazard analysis, in *Proceedings of the EERI 6th Seismic Zonation Workshop*, EERI, Palm Springs (California).
- Archuleta, R. J., and S. H. Hartzell (1981), Effects of fault finiteness on near-source ground motion, *Bulletin of the Seismological Society of America*, 71(4), 939–957, <https://doi.org/10.1785/BSSA0710040939>.
- Fujii, Yu., and K. Satake (2024), Slip distribution of the 2024 Noto Peninsula earthquake (MJMA 7.6) estimated from tsunami waveforms and GNSS data, *Earth, Planets and Space*, 76(1), <https://doi.org/10.1186/s40623-024-01991-z>.
- Hardin, B. O., and V. P. Drnevich (1972), Shear Modulus and Damping in Soils: Design Equations and Curves, *Journal of the Soil Mechanics and Foundations Division*, 98(7), 667–692, <https://doi.org/10.1061/JSFEAQ.0001760>.
- Ishikawa, Yu., and L. Bai (2024), The 2024 Mj7.6 Noto Peninsula, Japan earthquake caused by the fluid flow in the crust, *Earthquake Research Advances*, p. 100292, <https://doi.org/10.1016/j.eqrea.2024.100292>.
- Joyner, W. B., and T. F. Chen (1975), Calculation of nonlinear ground response in earthquakes, *Bulletin of the Seismological Society of America*, 65, 1315–1336, <https://doi.org/10.1785/BSSA0650051315>.
- NIED (2024), Realtime hazard information, <http://www.bosai.go.jp/e/index.html>.
- Pavlenko, O. V. (2008), Characteristics of Soil Response in Near-Fault Zones During the 1999 Chi-Chi, Taiwan, Earthquake, *Pure and Applied Geophysics*, 165(9–10), 1789–1812, <https://doi.org/10.1007/s00024-008-0401-1>.
- Pavlenko, O. V. (2016), Atypical soil behavior during the 2011 Tohoku earthquake ( $M_w = 9$ ), *Journal of Seismology*, 20(3), 803–826, <https://doi.org/10.1007/s10950-016-9561-0>.

- Pavlenko, O. V. (2017), Possible Mechanisms for Generation of Anomalously High PGA During the 2011 Tohoku Earthquake, *Pure and Applied Geophysics*, 174(8), 2909–2924, <https://doi.org/10.1007/s00024-017-1558-2>.
- Pavlenko, O. V. (2022), Influence of source directivity and site effects of 2003 Tokachi-oki earthquake on the generation of high PGA in the near-fault zones, *Scientific Reports*, 12(1), <https://doi.org/10.1038/s41598-022-16085-7>.
- Pavlenko, O. V., and K. Irikura (2003), Estimation of Nonlinear Time-dependent Soil Behavior in Strong Ground Motion Based on Vertical Array Data, *Pure and Applied Geophysics*, 160(12), 2365–2379, <https://doi.org/10.1007/s00024-003-2398-9>.
- Pavlenko, O. V., and K. Irikura (2006), Nonlinear Behavior of Soils Revealed from the Records of the 2000 Tottori, Japan, Earthquake at Stations of the Digital Strong-Motion Network Kik-Net, *Bulletin of the Seismological Society of America*, 96(6), 2131–2145, <https://doi.org/10.1785/0120060069>.
- Pavlenko, O. V., and V. A. Pavlenko (2023), Rupture Directivity Effects of Large Seismic Sources, Case of February 6th 2023 Catastrophic Earthquakes in Turkey, *Izvestiya, Physics of the Solid Earth*, 59(6), 912–928, <https://doi.org/10.1134/S1069351323060149>.
- Rosakis, A., M. Abdelmeguid, and A. Elbanna (2023), Evidence of Early Supershear Transition in the Feb 6th 2023 Mw 7.8 Kahramanmaraş Turkey Earthquake From Near-Field Records, *Preprint submitted to EarthArXiv*, <https://doi.org/10.31223/X5W95G>.
- Rowshandel, B. (2006), Incorporating Source Rupture Characteristics into Ground-Motion Hazard Analysis Models, *Seismological Research Letters*, 77(6), 708–722, <https://doi.org/10.1785/gssrl.77.6.708>.
- Shahi, S. K., and J. W. Baker (2011), An Empirically Calibrated Framework for Including the Effects of Near-Fault Directivity in Probabilistic Seismic Hazard Analysis, *Bulletin of the Seismological Society of America*, 101(2), 742–755, <https://doi.org/10.1785/0120100090>.
- Somerville, P. G., N. F. Smith, R. W. Graves, and N. A. Abrahamson (1997), Modification of Empirical Strong Ground Motion Attenuation Relations to Include the Amplitude and Duration Effects of Rupture Directivity, *Seismological Research Letters*, 68(1), 199–222, <https://doi.org/10.1785/gssrl.68.1.199>.